International Journal of Applied Electromagnetics and Mechanics
15th Int. Workshop on 1 & 2 Dimensional Magnetic Measurement and Testing, 2DM-Grenoble 24-26 Sept (2018) 1
IOS Press

Advanced iron-loss estimation for arbitrary magnetization loci in non-oriented electrical steel considering anisotropic effects

Benedikt Schauerte*, Simon Steentjes, Andreas Thul and Kay Hameyer
Institute of Electrical Machines (IEM), RWTH Aachen University, Schinkelstr. 4, Aachen, D-52062 Germany

Abstract. The design of electrical machines requires accurate models for the estimation of locally occurring iron losses. For this purpose, varieties of iron-loss models are proposed. These allow one to calculate iron losses as a function of the unidirectional peak flux density B_m and magnetization frequency f. Two-dimensional effects such as the materials' anisotropy and its influence on the loss behavior are neglected in most of these models, e.g., the dependency of the iron losses on the spatial loci of the magnetic field. Nonetheless, these effects have a considerable influence on the local iron-loss distribution. Measurements under vector-field conditions, which consider the flux loci and the magnetic anisotropy, along with modeling approaches to replicate the behavior are presented in this work.

Keywords: iron loss modeling, vector hysteresis, magnetic anisotropy

1. Introduction

In order to allow an improved design and better thermal layout of rotating electrical machines, a variety of iron-loss models, which are able to predict the occurring iron losses at different operation points with respect to the peak flux density and magnetization frequency, have been developed [1,2]. Due to the trend of increasing operation speeds and higher magnetic utilization in the design of electrical machines, several adjustments have been performed on these models, in order to enhance the validity of the models in these ranges [3,4]. Despite the increasing validity of these loss formulations, the models are parameterized mostly based on measurements of unidirectional flux densities and, as a result, the models are only suitable for modelling iron losses caused by these magnetization forms. Nonetheless, the magnetic flux paths in rotating electrical machines often differ strongly from these classically examined waveforms, such as e.g. elliptical and rotational field loci that have a significant influence on the resulting iron-loss distribution [5]. Measurement devices that allow the measurement and analysis of the materials' characteristics under two-dimensional excitations of different spatial forms are designed and put into operation [6-8].

The occurring iron losses at rotational magnetizations behave decisively different with higher losses in the regions of lower magnetizations and reduced losses at saturation. The transition between the behaviour of uniaxial and rotational magnetization is ambiguous depending on axis ratio f_{Ax} and across all attained states of saturation of the respective material. The parameter f_{Ax} describes the ratio between the main and the transverse components of the B-Loci, starting at 0 for unidirectional curves and then increasing with widening up ellipsoids until an axis ratio of 1 denotes circular magnetization. This paper presents an extension of the existing parametrical loss formulations to two-dimensional field curves taking into consideration the respective spatial waveform, such as the inclination angle of the magnetization with respect to the rolling direction (RD) based on one-dimensional material measurements.

*Corresponding author: Benedikt Schauerte, Institute of Electrical Machines (IEM), RWTH Aachen University, Schinkelstr. 4, Aachen, D-52062 Germany

The statistical loss separation theory (SLT) introduced by Bertotti, is used to determine the influence of rotating magnetizations on the individual loss components and their quantity as a function of the frequency and the materials' saturation state. The influence of saturation effects on iron losses under rotating magnetizations is taken into account here via an averaged magnetization characteristic of the respective material, which was determined at different angles to the rolling direction.

2. Iron loss separation

For one-dimensional sinusoidal magnetizations, iron losses can be identified with standardized one-dimensional measurement devices such as the single-sheet-tester (SST) or the Epstein frame. For such magnetizations, the SLT to separate the occurring losses in hysteresis, classical eddy-current and excess losses has proven to be valid. Given a set of measurements and some basic material characteristics, a mathematical formulation of the iron losses as a function of the peak flux density B_{m} and the frequency f can be derived:

$$P_{\mathrm{Fe}}(f, B_{\mathrm{m}}) = k_{\mathrm{hyst}}\, B_{\mathrm{m}}^{\alpha}\, f + k_{\mathrm{cl}}\, B^2 f^2 + k_{\mathrm{exc}}\, B^{1.5} f^{1.5} \qquad (1)$$

In general, the approach is based on the separation of the occurring iron losses into three different loss components [1]. The hysteresis losses are linked to the energy-loss that occur during the domain wall movement. They are static with respect to the applied frequency and depend only on the peak value of the magnetic flux density. In most formulations, this loss component is strictly homogeneous increasing under the neglecting of saturation effects at higher peak flux densities.

The excess loss component P_{exc} represent the influence of local occurring eddy currents that are induced by the change of the magnetic flux during the movement of the domain walls.

The classical eddy-current losses are evoked by global eddy currents that occur along the materials' cross section oriented according to Lenz's law against the applied field. Their dependency of the applied magnetization frequency and peak flux density are derived by the Maxwell equations. The parameter for the classical eddy currents k_{cl} can be derived by the materials' conductivity ρ_{e}, sheet thickness d and the specific mass density ρ: $\pi^2 d^2 / 6\rho_{\mathrm{e}}\rho$. The other model parameters k_{hyst}, k_{exc} and the exponential hysteresis loss exponent α are identified by error minimization methods and then kept constant for the entire range of operation point. It should be noted that in an adjusted formulation of this approach, the classical eddy-current coefficient k_{cl} is also defined during a parameter fitting, as the analytic formulation is based on the assumption, that the field inside the electrical steel sheet only has small deviations to the applied field. Regarding the excess loss parameter k_{exc} it is suggested in some works, to introduce a dependency of the parameter from the peak flux density B_{m} as the distance, and with it the locally induced voltage at the abrupt movements of the domain walls depend on the amplitude of the controlled magnetic flux density [8]. The input variables are the peak flux density and the magnetic fundamental frequency f, distortion effects or higher harmonics are not considered in this simple formulation of the Bertotti-model.

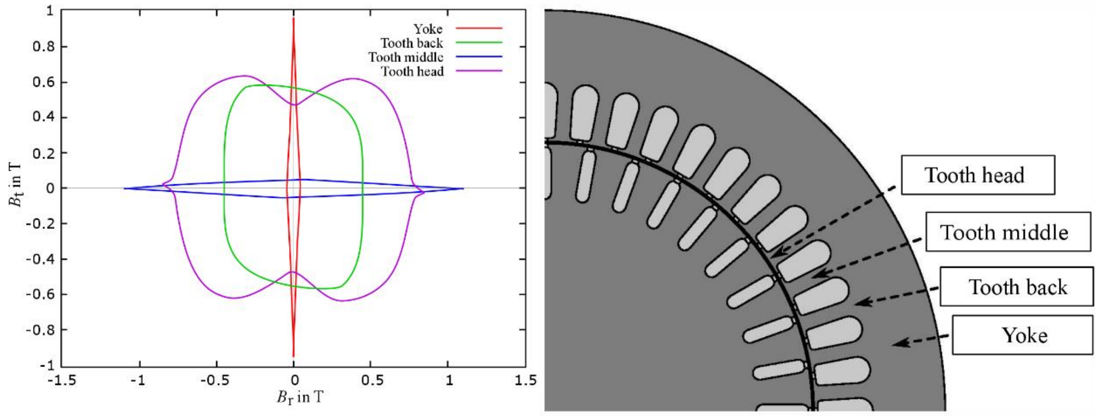

Fig. 1: Spatial magnetic flux density loci described in radial and tangential components B_{r} and B_{t} at different points as indicated on the right. [10]

3. Iron loss at two-dimensional magnetization

As mentioned before, the spatial loci of the magnetic flux density in rotating electrical machines strongly depends on the position of the examined spatial point in the steel laminations' cross section. In the middle of the stator and rotor teeth and the center of the yoke almost unidirectional flux density curves occur, which can be considered with good accuracy by the iron-loss models presented in the previous section. Another behavior is present for the tip and back of the teeth. For the case of an induction machine in both, rotor and stator elliptical and circular field-loci occur. For a pmsm, rotating magnetization loci only occur on the stator side, due to the nearly constant magnetic flux density inside the rotor lamination, preserved by the permanent magnets. Exemplarily flux density loci at different points on the laminations cross section are depicted in Fig. 1.

Nonetheless, for both machine types, a considerable ratio of the laminations cross section is facing spatial magnetic flux density loci which strongly differ from the typically examined one-dimensional waveforms. For the case of such arbitrary waveforms, the field loci can be interpreted in a first order approximation as circular and elliptical magnetic flux loci with ambiguous transitions. For the measurement of the occurring iron losses under rotational magnetizations rotational single sheet testers (RSST) were designed, which allow the examination of the magnetic behavior and the resulting iron losses under unidirectional, elliptical and rotational magnetizations. The RSST used in this work is presented in detail in [6]. Even though these devices partly strongly differ in terms of construction, magnetic circuits and the utilized techniques for the measurement of the magnetic field properties, the resulting measured iron losses show similar behavior. Independent of the respective chosen measurement device, the performed iron loss measurements reveal considerable deviations between unidirectional and vectoral flux density loci, which have to be taken into account for an exact prediction of the machine behavior and the iron-loss distribution across the steel laminations.

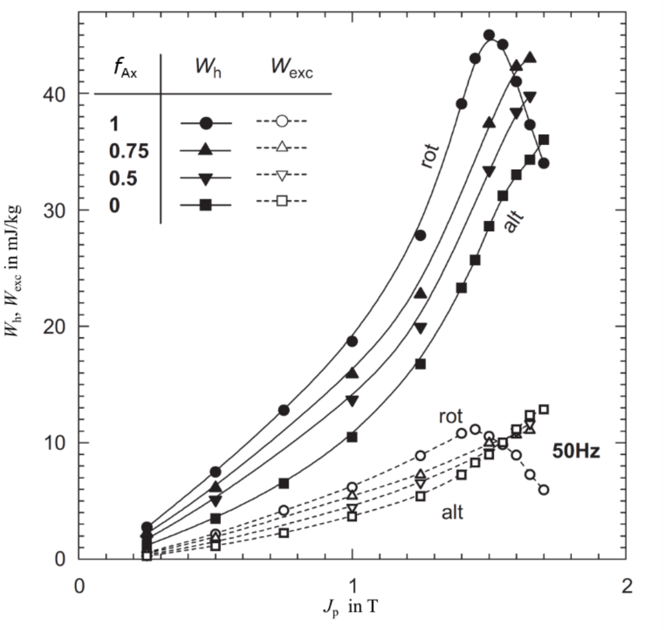

Fig. 2: Hysteresis and excess loss components for axis ratios 0, 0.5, 0.75 and 1.0 at 50 Hz [11].

In Fig. 2, the behavior of the hysteresis and excess loss components P_{hyst} and P_{exc} which are linked to the motion of the domain walls, are depicted for unidirectional, circular and elliptical B-loci of different axis ratios. In the region of low flux density, the loss components are increasing homogenously with the axis ratio, with a factor of almost 2.5 between circular and unidirectional magnetizations. The transition to the saturated state reverses this behavior. The slope of the losses decreases for the two elliptic magnetization loci, the losses measured at circular magnetizations decline as the peak flux density approaches the saturation polarization J_{S}. Iron loss measurements with thermometric methods revealed that the hysteresis and excess loss components nearly decrease to zero for circular magnetizations as presented in [9]. This behavior can be explained by the decrease of domain-wall motions when the energy of the applied field grows strong enough to overcome the magneto-crystalline anisotropy energy of the iron crystals. Therefore, the domain-wall movements subside until, theoretically at the fully saturated state, big domains just rotate with the applied magnetic field and both domain movement linked loss components diminish completely.

4. Loss model

In order to provide an accurate description of the resulting iron losses, which occur during the operation of rotating electrical machines, a suitable loss model has to take into account next to the classically considered magnetic flux density B and magnetization frequency f also the respective spatial shape of the magnetic flux density. This can be taken into account by the axis ratio f_{Ax} and the inclination angle θ, which represents the displacement of the examined B-loci's inclination angle. The interpretation of the four input variables of the loss model are depicted schematically in Fig. 3. For the consideration of f_{Ax}, the authors of [9-11] introduce rotational loss factors r_{hyst} and r_{exc} , which are suggested to be homogeneously decreasing by the peak flux density B_{m}. As an extension to this empirical approach, this paper presents a loss formulation based on unidirectional measurements at different angles to the rolling direction. The rotational loss parameters r_{hyst} and r_{exc} are retained but defined as a function of an average magnetization characteristic of the material to take into account the saturation-dependence of the iron losses at rotating magnetizations.

$$P_{\mathrm{Fe}}(f, \theta, f_{\mathrm{Ax}}, B_{\mathrm{m}}) = P_{\mathrm{hyst}} + P_{\mathrm{cl}} + P_{\mathrm{exc}} \qquad (3)$$

With the components:

$$P_{\mathrm{hyst}} = (1 - f_{\mathrm{Ax}}^2 r_{\mathrm{hyst}})(k_{\theta,\mathrm{hyst}} B_{\mathrm{m}}^2 + k_{\theta+90°,\mathrm{hyst}} (f_{\mathrm{Ax}} B_{\mathrm{m}})^2) f \qquad (4)$$

$$P_{\mathrm{exc}} = (1 - f_{\mathrm{Ax}}^2 r_{\mathrm{exc}})(k_{\theta,\mathrm{exc}} B_{\mathrm{m}}^{1.5} + k_{\theta+90°,\mathrm{exc}} (f_{\mathrm{Ax}} B_{\mathrm{m}})^{1.5}) f^{1.5} \qquad (5)$$

$$P_{\mathrm{cl}} = (B_{\mathrm{m}}^2 + (f_{\mathrm{Ax}} B_{\mathrm{m}})^2) k_{\mathrm{cl}} f^2 \qquad (6)$$

With the rotational loss parameters r_{hyst} and r_{exc} defined by a mathematical transformation of the magnetization curve:

$$r_{\mathrm{hyst,exc}} = B_{\mathrm{m}}(B_{\mathrm{scale}})/B_{\mathrm{S}} \qquad \text{with} \qquad B_{\mathrm{scale}} = B_{\mathrm{m}} \cdot \frac{H_{\mathrm{m}}}{H_{\mathrm{S}}} \qquad (7)$$

The influence of the materials saturation status can be taken into account. By the scaling on the respective peak value of the magnetic field the saturation directly influences the two affected loss components P_{hyst} and P_{exc}. All loss components and their calculation are based on a vector separation of the magnetic flux density into main- and cross-component of the respective loci. The dependence of the domain mobility is influenced by the crystallographic structure and, thus, the magnetic anisotropy. Consequently, the calculation of the hysteresis and excess loss components is based on inclination angle-dependent parameters, in order to take into account this anisotropic behavior [12]. The multiplication with f_{Ax}^2 ensures the gliding transition between uniaxial and rotational magnetizations as depicted for hysteresis- and excess

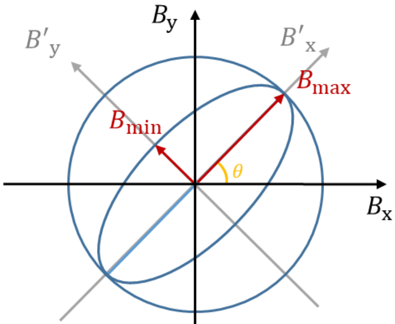

Fig. 3: Definition of the relevant variables for the iron loss calculation θ, f_{Ax} and B_m. The maximal flux density B_m is multiplied with f_{Ax} to create the respective loop shape. The resulting ellipsoid is then rotated by θ. The new main- (B'_x) and cross-axis (B'_y) of the resulting ellipsoid are depicted in grey.

component in Fig. 4. The exponent 2 can be interpreted later as a model parameter, for the time being it is set constant. The index θ describes the inclination angle of the ellipsoids' main axis, thus θ+90° denotes the parameters identified for the respective cross direction. By this means, the materials anisotropy in terms of iron loss is considered. The model parameters $k_{\theta,\mathrm{exc}}$ and $k_{\theta,\mathrm{hyst}}$ are identified by unidirectional loss measurements performed at different angles θ to the rolling direction of the material. To take into account the additional iron losses evoked by the elliptical magnetization in the transverse direction of the rotated main axis $\mathrm{B'_x}$, the orthogonal loss parameters of the magnetization in $\mathrm{B'_y}$ are taken into account, denoted by +90° in the indices. For the classical eddy-current losses, a consideration of the material parameters with respect to the angle to the rolling direction θ is not necessary, as the electrical conductivity of the material can be assumed to be independent of the angle. The physical interpretation of the parameters is similar to their definition in the classical Bertotti loss model.

5. Results

The resulting iron-loss components for a fully processed non-oriented electrical steel with a thickness of 0.5 mm and a silicon content of 2.4 wt.% at a magnetization frequency of 200 Hz are presented in Fig. 4. The transition from the well-studied iron loss for unidirectional behavior to higher iron losses at low magnetizations, which decrease in the saturation region for circular magnetizations, can be seen for the hysteresis and excess loss components. For flux densities below 1.0 T the material is still in its linear region and due to the inclusion of the magnetization curve into the loss-formulation, the loss-reducing rotational factors do not have a considerable influence. At higher flux densities close, to the saturation polarization the losses decrease to zero for circular *B*-loci as evidently follows from mathematical formulation. For an accurate recreation of the transition of the saturations' influence with respect to the axis ratio as more detailed examination of the fundamental phenomena must be carried out.

Regarding the classical eddy current loss components, a more distinct behavior is visible. As the sum of the vector components increases with the f_{Ax} and no nonlinearities as saturation effects have to be taken into account, the simulation yields a homogeneous gradient with respect to both variables f_{Ax} and

In general, the proposed model is able to replicate the observed behavior based only on mathematical adjustments of Bertotti's loss formula. After a suitable parameter identification procedure, the loss components can be examined and utilized more detailed insights on the material behavior and iron loss distribution in the machine application. No quantities like rotational excess and loss factors with arbitrary slopes that only depend on parameter identification methods of measured behavior are included. For the case of additionally distorted magnetic flux-loci, which differ in their shape from the circular spatial curves studied in this work the proposed formulas can be extended by the Fourier coefficients of the respective curves. For future work the influence of a constant DC-offset, which displaces the center of the respective examined flux density loci, on the iron losses has to be examined and included into the models' scope. In Fig. 5 the simulation results for measured rotational losses with different B-loci are presented. The measurements were performed at 200 and 400 Hz with the main axis oriented collinear to the rolling direction. For the identification of the loss parameters unidirectional measurements in rolling and transverse direction were performed at 50, 100, 200 and 400 Hz. For the identification of the parameters and the simulation of the resulting losses, the software Matlab was used. The model is able to recreate the measured behavior at different spatial field loci with good accuracy. The performed measurements are limited in terms of the maximum reachable magnetization level and the lowering of the magnetization frequency. The field control of the device and thus the form factor of the individual

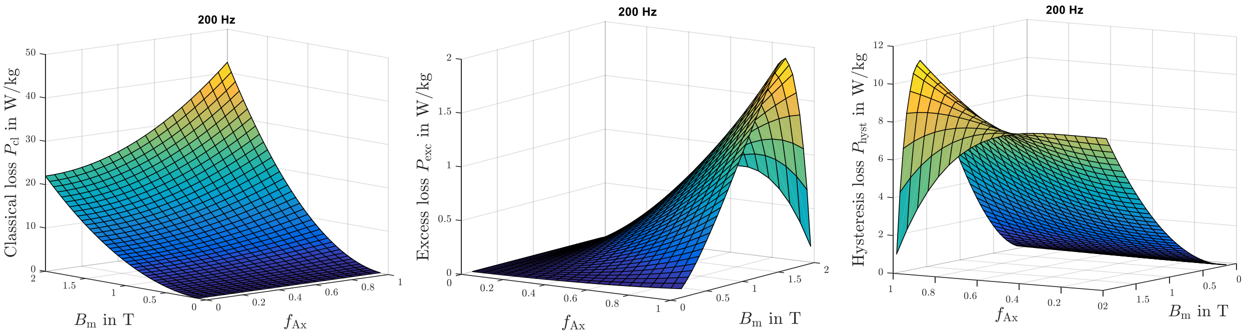

Fig. 4: Iron loss components with respect to magnetic peak flux density B_m and axis ratio f_{Ax} at 200 Hz with 0° inclination angle to the rolling direction.

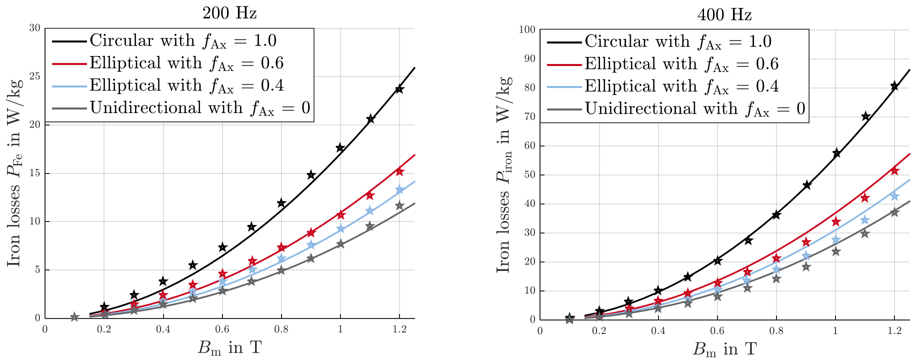

Fig. 5: Measured (dotted) and simulated (continuous) iron losses at 200 and 400 Hz at different axis ratios. The main axis is perpendicular to the rolling direction. The measurements were performed on a RSST presented in [6].

vector components, which is decisive for an exact loss determination, suffers from a violation of the aforementioned boundary conditions.

6. Conclusions

In general, the proposed model is able to replicate the observed behavior based only on mathematical adjustments of Bertotti's loss formula. After a suitable parameter identification procedure, the loss components can be examined and utilized more detailed insights on the material behavior and iron loss distribution in the machine application. No quantities like rotational excess and loss factors with arbitrary slopes that only depend on parameter identification methods of measured behavior are included. For the case of additionally distorted magnetic flux-loci, which differ in their shape from the circular spatial curves studied in this work the proposed formulas can be extended by the Fourier coefficients of the respective curves. For future work, loss measurements at higher magnetic flux densities and the influence of a constant DC-offset, which displaces the center of the respective examined flux density loci, on the iron losses needs to be examined and included into the models' scope.

Acknowledgements

The work of Benedikt Schauerte is performed in the research project group project "SPP-2013 - The utilization of residual stresses induced by metal forming funded by the Deutsche Forschungsgesellschaft (DFG) HA 4395/22-1 as DFG 255713208.

References

[1] Bertotti, G. (1988). General properties of power losses in soft ferromagnetic materials. IEEE Transactions on magnetics, 24(1), 621-630.
[2] Gmyrek, Z., Boglietti, A., & Cavagnino, A. (2010). Estimation of iron losses in induction motors: Calculation method, results, and analysis. IEEE Transactions on Industrial Electronics, 57(1), 161-171.
[3] Steentjes, S., von Pfingsten, G., Hombitzer, M., & Hameyer, K. (2013). Iron-loss model with consideration of minor loops applied to FE-simulations of electrical machines. IEEE Transactions on Magnetics, 49(7), 3945-3948.
[4] Eggers, D., Steentjes, S., & Hameyer, K. (2012). Advanced iron-loss estimation for nonlinear material behavior. IEEE Transactions on Magnetics, 48(11), 3021-3024.
[5] Moses, A. J. (1992). Importance of rotational losses in rotating machines and transformers. Journal of Materials Engineering and Performance, 1(2), 235-244.
[6] Thul, A., Steentjes, S., Schauerte, B., Klimczyk, P., Denke, P., & Hameyer, K. (2018). Rotating magnetizations in electrical machines: Measurements and modeling. AIP Advances, 8(5), 056815.
[7] Ragusa, C., Zurek, S., Appino, C., & Moses, A. J. (2008). An intercomparison of rotational loss measurements in non-oriented Fe–Si alloys. Journal of Magnetism and Magnetic Materials, 320(20), 623-626.
[8] Kowal, D., Sergeant, P., Dupré, L., & Vandenbossche, L. (2015). Comparison of iron loss models for electrical machines with different frequency domain and time domain methods for excess loss prediction. IEEE Trans. Magn, 51(1), 1-10.
[9] Appino, C., Fiorillo, F., & Ragusa, C. (2009). One-dimensional/two-dimensional loss measurements up to high inductions. Journal of Applied Physics, 105(7), 07E718.
[10] Steentjes, S., Leßmann, M., & Hameyer, K. (2012, October). Advanced iron-loss calculation as a basis for efficiency improvement of electrical machines in automotive application. In Electrical Systems for Aircraft, Railway and Ship Propulsion (ESARS), 2012 (pp. 1-6). IEEE. [5] Dicnamesta 44(3), 222–263.
[11] Ragusa, C., C. Appino, and F. Fiorillo. "Magnetic losses under two-dimensional flux loci in Fe–Si laminations." Journal of magnetism and magnetic materials 316.2 (2007): 454-457.
[12] Tumanski, S. (2003). Investigations of the anisotropic behaviour of SiFe steel. Journal of Magnetism and Magnetic Materials, 254, 50-53.